EXAMINATION ON CONSECUTIVE RUPTURING OF TWO CLOSE FAULTS BY DYNAMIC SIMULATION

M. Muto[1], K. Dan[1], H. Torita[1], Y. Ohashi[1], and Y. Kase[2]

[1] *Ohsaki Research Institute, Inc., Tokyo, Japan*
[2] *National Institute of Advanced Industrial Science and Technology, Ibaraki, Japan*
Email: muto@ohsaki.co.jp, kazuo.dan@ohsaki.co.jp, torita@ohsaki.co.jp, ohashi@ohsaki.co.jp, kasep@ni.aist.go.jp

ABSTRACT :
It is necessary to judge whether the active faults located closely to each other will rupture together or independently for predicting the magnitude and the probability of the next earthquake. In this paper, we carried out some basic examinations on the consecutive rupturing of the two adjacent active faults by the dynamic rupture simulation based on the slip-weakening model. Our results showed that the following conditions were needed for the second fault to rupture completely after the first left-lateral fault ruptured: 1) lower strength excess normalized by dynamic stress drop, 2) narrower depth and smaller negative stress drop of the inactive area between the two faults, and 3) right step of the second fault rather than left step.

KEYWORDS:
Consecutive Rupturing, Fault Distance, Dynamic Rupture Simulation, Slip-Weakening Model, Strength Excess

1. INTRODUCTION

It is an important subject to interpret the relationship between the active fault observed on the ground surface and the seismic source fault deep under the ground surface for predicting the strong motions and the crustal deformations caused by a scenario earthquake. Especially, it is necessary to judge whether the active faults located closely to each other will rupture together or independently for predicting the magnitude and the probability of the next earthquake.
The mechanical property and the geometry of the fault are principal factors governing the consecutive fault rupturing. The strength excess, the stress drop, and the critical displacement characterize the fault rupture mechanism, and govern fragility at every local part of the fault. Moreover, the fault geometry affects the stress changing around the fault after rupturing, and induces the consecutive rupturing of the adjacent fault.
A lot of examinations concerning the consecutive rupturing have been studied by numerical simulation based on the slip-weakening model for the stress-displacement relation on the fault plane. However, most of these examinations describe the simulation of the specific fault rupturing, and few of them systematically describe the effect of the mechanical property and the fault geometry on the consecutive rupturing.
In this paper, we systematically examined the effect of the strength excess, the area and the negative stress drop on the inactive area between the two faults, and the step direction and the distance between the two faults on the consecutive rupturing by the dynamic simulation based on the slip-weakening model.

2. SLIP-WEAKENING MODEL AND ITS PARAMETERS

Figure 1 shows the coordinate system, and Figure 2 shows the slip-weakening model used in this paper. In Figure 1, the directions of the tectonic stress (σ_1, σ_2, σ_3) are taken to be the same directions as those of the coordinate system (X, Y, Z). Here, σ_1 is the east-west direction stress, and σ_2 is the south-north direction stress. The fault plane and its normal vector construct the coordinate system (x, y, z). Here, the tectonic stress is assumed to be the east-west compression as in Japan. The analysis was carried out by the three dimensional finite difference method, which was developed by Kase and Kuge (2001).
The analysis region was x=135 km long, y=60 km wide, and z=45 km deep within about 30 km from the fault. The finite difference grid interval Δx was 0.25 km in each direction. The initial rupture area was 3.25 km by 3.25 km. The density ρ was 2.7 g/cm^3, the P-wave velocity α was 6.0 km/s, and the S-wave velocity β was 3.5

km/s. The duration was 30 seconds, and the time interval was 0.025 seconds.
The tectonic stresses σ_1 and σ_2 were determined by eqs. (2.1) and (2.2) of Kase (2002). In these equations, the average depth of the fault, 7.5 km (the half of the seismogenic layer, 15 km) was substituted for Z[km]. Because we only examined vertical strike-slip faults in this study, σ_3 was not related to the simulation result, and then set to be 0 MPa.

$$\sigma_1 = \sigma_{max}\,[\mathrm{MPa}] = 42\,Z[\mathrm{km}] + 6 \quad (2.1)$$
$$\sigma_2 = \sigma_{min}\,[\mathrm{MPa}] = 20\,Z[\mathrm{km}] + 2 \quad (2.2)$$

The fault strike was set to be 45° clockwise, because we examined northwest-southeast-direction faults. This assumption represented the left-lateral slip because the faults were in the east-west compressional field.
The dynamic stress drop $\Delta\sigma_d$ was assumed to be 4 MPa. It was determined by the empirical relation between the fault area S [km^2] and the seismic moment M_0 [dyne−cm] of Irikura and Miyake (2001) by eq. (2.3) and the theortical relation of Eshelby (1957) among the stress drop $\Delta\sigma_s$, the seismic moment M_0, and the fault area S of the circular crack by eq. (2.4).

$$M_0 = \{S/(4.24\times10^{-11})\}^2 \text{ for } M_0 \text{ larger than } 7.5\times10^{25} \text{ dyne-cm} \quad (2.3)$$
$$\Delta\sigma_s = (7\pi^{1.5}/16)(M_0/S^{1.5}) \quad (2.4)$$

Here, we assumed $\Delta\sigma_d = \Delta\sigma_s$ and the fault area = 1,000 km^2.
The strength excess SE was assumed to be SE=1.6$\Delta\sigma_d$ for the fundamental case. This is because the resultant rupture velocity does not exceed the S-wave velocity and the rupture propagates stably when the strength excess SE is about 1.6 times the dynamic stress drop $\Delta\sigma_d$ (Andrews, 1976).
We adopted 0.25 m as the critical distance D_c. This is because the critical distance D_c has a relation with the rupture front length L_c in the case of a two dimensional shear crack by eq. (2.5) according to Andrews (1976) and L_c must be about $8\Delta x$ = 2 km in order to calculate the homogeneous fault with the analysis code used in this study.

$$L_c = \frac{2\mu(\lambda+\mu)(\sigma_s-\sigma_d)}{\pi(\lambda+2\mu)(\sigma_0-\sigma_d)^2}D_c \quad (2.5)$$

Here, λ and μ are Lame's constant.
Table 1 shows the parameters of the slip-weakening model used in this paper.

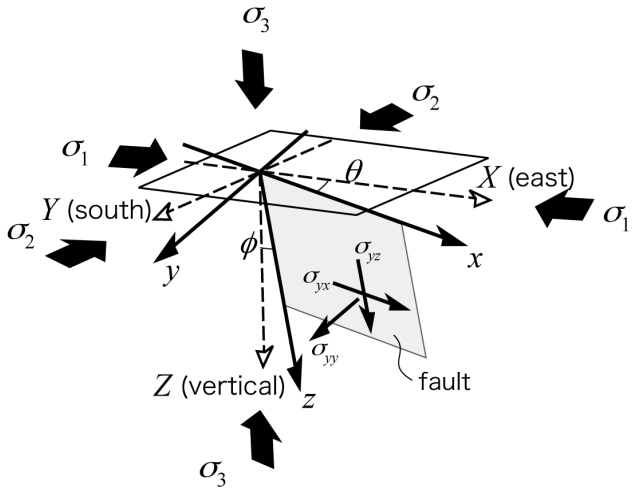

Fig. 1. Coordinates used in this paper.

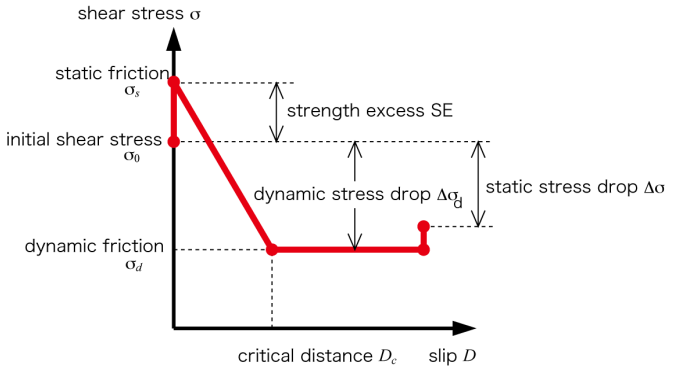

Fig. 2. Slip-weakening model used in this paper.

Table 1. Parameters of the slip-weakening model used in this paper.

tectonic stress	σ_1	321 MPa	$\sigma_{max} = 42Z$[km]+6 (Kase, 2002)
	σ_2	152 MPa	$\sigma_{min} = 20Z$[km]+2 (Kase, 2002)
	σ_3	0 MPa	
fault angle to X axis	θ	45°	left lateral slip
fault angle to Z axis	ϕ	0°	vertical fault
dynamic stress drop	$\Delta\sigma_d$	4 MPa	eqs.(2.3) and (2.4) in the text
initial stress	σ_{yy}	-236.5 MPa	$\sigma_{yy}=(\sigma_1\sin^2\theta+\sigma_2\cos^2\theta)\cos^2\phi+\sigma_3\sin^2\phi$
	σ_{yx}	84.5 MPa	$\sigma_{yx}=(-\sigma_1+\sigma_2)\sin\theta\cos\theta\cos\phi$
	σ_{yz}	0 MPa	$\sigma_{yz}=(-\sigma_1\sin^2\theta-\sigma_2\cos^2\theta+\sigma_3)\sin\phi\cos\phi$
initial shear stress	σ_0	84.5 MPa	$\sigma_0=(\sigma_{yx}^2+\sigma_{yz}^2)^{1/2}$
strength excess	SE	6.4 MPa	$SE=1.6\Delta\sigma_d$ for the initial model
critical distance	D_c	0.25 m	eq. (2.5) in the text
density	ρ	2.7 g/cm^3	
P-wave velocity	α	6.0 km/s	
S-wave velocity	β	3.5 km/s	

3. THE EFFECT OF THE DIFFERENCE OF THE SLIP-WEAKENING PARAMETERS TO CONSECUTIVE RUPTURING

In order to investigate the effect of the difference of the slip-weakening parameters to the consecutive rupturing, we changed the strength excess SE. For easy comparison among the results of the different strength excesses, we introduced a nondimensional parameter of the $R(\sigma_s)$ defined by

$$R(\sigma_s) = \frac{\sigma_s - \sigma_0}{\Delta\sigma_d}. \tag{3.1}$$

Figure 3(a) shows the slip-weakening model used in past references. The horizontal axis represents the slip displacement, and the longitudinal axis represents the shear stress normalized by the following equation:

$$R(\sigma) = \frac{\sigma - \sigma_0}{\Delta\sigma_d}. \tag{3.2}$$

Figure 3(b) shows the critical distance D_c and the $R(\sigma_s)$ in each slip-weakening model shown in Figure 3(a). The critical distance D_c in the past references is from 0.1 to 0.8 m. The $R(\sigma_s)$ is from 0 to 2.5. Based on these data, we adopted the 1.6, 1.0, and 0.5 as the $R(\sigma_s)$ in this study.

We assumed the length of the first fault to be 30 km, and that of the second fault to be 20 km. Because the distance between two faults is known as the important parameter for the consecutive rupturing, the distance was changed to be 2, 3, and 5 km.

Figure 4 shows the effect of the $R(\sigma_s)$ with 5-km fault distance. Figure 4(a) is the result of the case of $R(\sigma_s)$=1.0, and Figure 4(b) is the result of the case of $R(\sigma_s)$=0.5. If the $R(\sigma_s)$ decreased, the consecutive rupturing was easy to occur. The smaller the $R(\sigma_s)$ was, the faster the rupture velocity became, and the rupture velocity was easy to exceed the S-wave velocity.

Table 2 summarizes the parameters for all the cases examined in this study and the results of the consecutive rupturing. These results show that the consecutive rupturing occurred even with a long distance between the two faults when the $R(\sigma_s)$ was small enough.

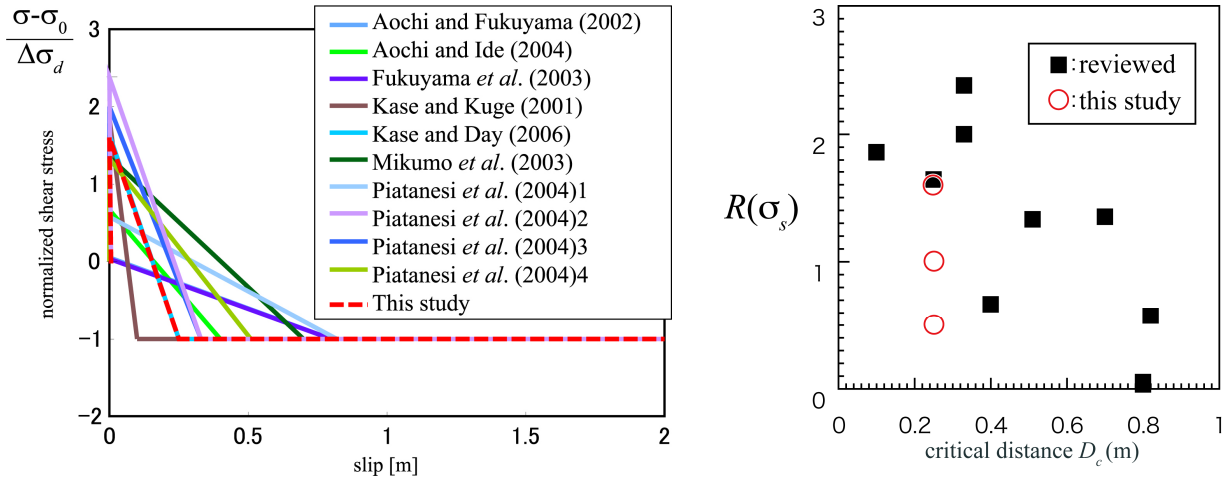

(a) Slip-weakening models (b) $R(\sigma_s)$ and D_c

Fig. 3. Slip-weakening models for the examination of the effect on their consecutive rupturing.

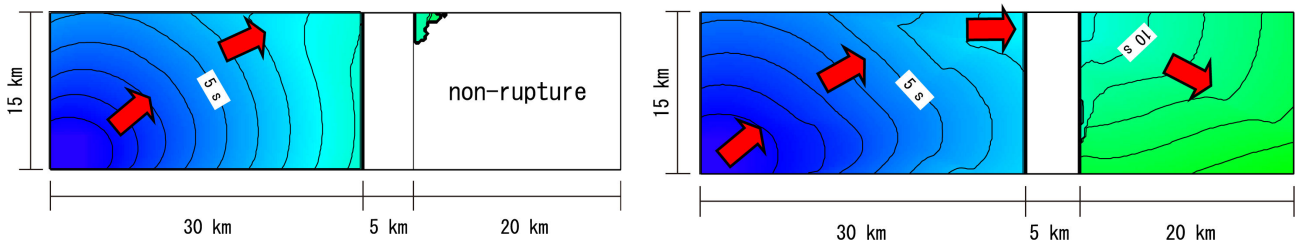

(a) $R(\sigma_s)$=1.0 (b) $R(\sigma_s)$=0.5

Fig. 4. The effect of the strength excess on the consecutive rupturing (fault distance = 5 km)

Table 2. Parameters of the models for the examination of the effect of the strength excess on the consecutive rupturing and the results.

fault distance	$R(\sigma_s)=SE/\Delta\sigma_d$	result	Figure
2 km	1.6	single rupture	-
	1.0	consecutive rupture	-
	0.5	consecutive rupture	-
3 km	1.6	single rupture	-
	1.0	consecutive rupture	-
	0.5	consecutive rupture	-
5 km	1.6	single rupture	-
	1.0	single rupture	Fig. 4(a)
	0.5	consecutive rupture	Fig. 4(b)

4. RUPTURE PROPAGATION ON THE FAULT SYSTEM INCLUDING INACTIVE AREA

Next, we examined the effect of the inactive area between the two faults on the consecutive rupturing. Here, we assumed the length of the inactive area to be 5 km and the width to be 5 km and 15 km as shown in Figure 5. Moreover, we assumed the dynamic stress drop $\Delta\sigma_d$ on the inactive area to be negative. Concretely speaking, as shown in Figure 6, the strength excess SE on the inactive area was assumed to be the same as that on the active region SE^* (6.4 MPa) and the dynamic stress drop $\Delta\sigma_d$ on the inactive area to be -0.5, -1.0, and -0.5 times $\Delta\sigma_d^*$ (4 MPa) on the active region.

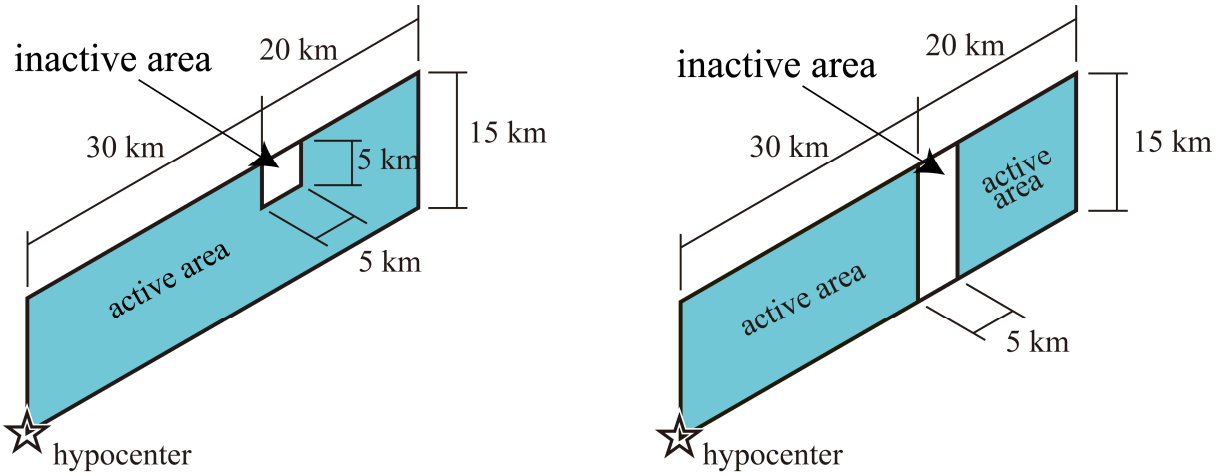

(a) The 5-km width model (b) The 15-km width model

Fig. 5. Models of the fault system including the inactive area.

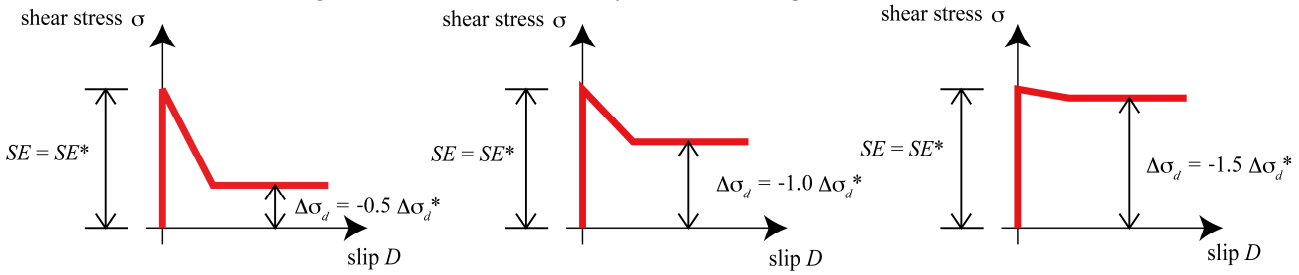

(a) Model A (b) Model B (c) Model C

Fig. 6. Slip-weakening models of the inactive area. Here, *SE** is the strength excess of the active area, and $\Delta\sigma_d$* is the dynamic stress drop of the active area.

Figure 7 shows the results for the model B for the inactive area. Figure 7(a) shows the result including the inactive area of the 5-km width. It shows the decrease of the rupture velocity on the inactive area but the complete rupture on the entire fault. On the other hand, Figure 7(b) shows the result including the inactive area of the 15-km width. It also shows the decrease of the rupture velocity on the inactive area and the pause of the rupture propagation in deep region.

Figure 8 shows the results for the model C. Figure 8(a) shows the result for the inactive area of the 5-km width. This is little different from the results for model B (Figure 7(a)). Figure 8(b) shows the result including inactive area of the 15-km width. The rupture did not propagate beyond the inactive area.

Table 3 summarizes the parameters for all the cases examined in this study and the results of the consecutive rupturing. These results indicate shallower limitation and smaller negative stress drop on the inactive area between the two faults are needed for the rest of the first fault or the second fault to rupture completely.

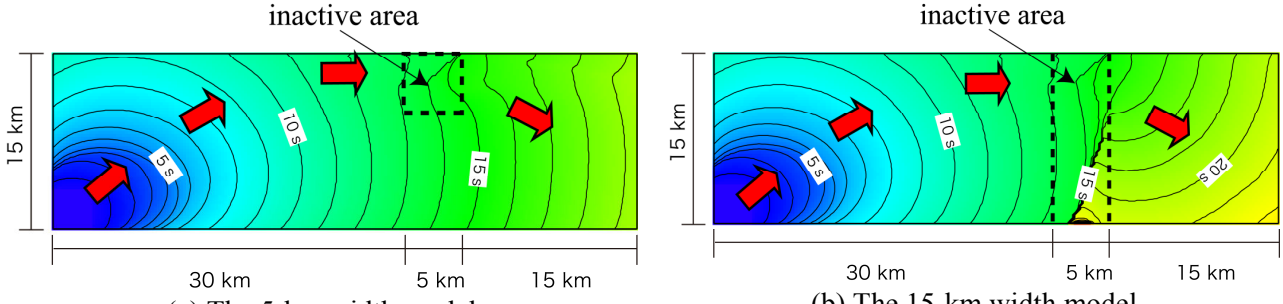

(a) The 5-km width model (b) The 15-km width model

Fig. 7. The effect of the width and the negative stress drop of the inactive area between the active faults on the consecutive rupturing. Here, Model B is used as the slip-weakening model of the inactive area.

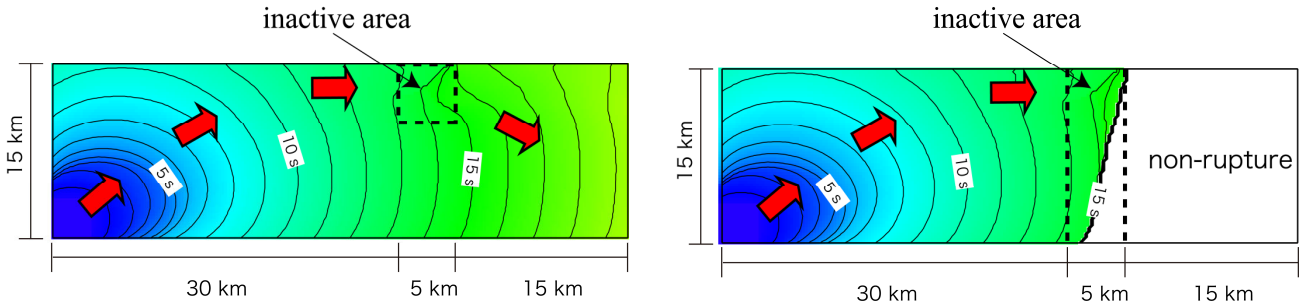

(a) The 5-km width model (b) The 15-km width model

Fig 8. The effect of the width and the negative stress drop of the inactive area between the active faults on the consecutive rupturing. Here, Model C is used as the slip-weakening model of the inactive area.

Table 3. Parameters of the models of the fault systems including the inactive area and the results. Here, $\Delta\sigma_d^*$ is the dynamic stress drop of the active area.

width of the inactive area	$\Delta\sigma_d/\Delta\sigma_d^*$	result	Figure
5 km	-0.5	consecutive rupture	-
	-1.0	consecutive rupture	Fig. 7(a)
	-1.5	consecutive rupture	Fig. 8(a)
15 km	-0.5	consecutive rupture	-
	-1.0	consecutive rupture	Fig. 7(b)
	-1.5	single rupture	Fig. 8(b)

5. THE EFFECT OF RELATIVE POSITION OF TWO PARALLEL FAULTS TO THE CONSECUTIVE RUPTURING

Finally, we examined the effect of the step direction of the second fault from the first fault on the consecutive rupturing. We assumed the left step of 0.75 km and the right step of 0.75 km, and the distance between two faults of 0, 2, 5, and 10 km. Here, the strength excess *SE* was assumed to be 4 MPa which was the same as the dynamic stress drop $\Delta\sigma_d$. Table 4 summarizes the parameters and the results.

Figure 9(a) shows the result of the left step with the 5-km fault distance. The rupture did not propagate on the second fault, but we can see a small area of rupturing. On the other hand, Figure 9(b) is the result with the 2-km fault distance, and shows that the second fault ruptured completely by the decrease of the fault distance.

Figure 9(c) shows the result of the right step with the 5-km fault distance. The consecutive rupturing occurred in this case. On the other hand, Figure 9(d) shows the result of the right step with the 10-km fault distance. In this case, the rupture of the first fault did not affect on the rupture of the second fault because of the large fault distance.

Table 4. Parameters of the models for the examination of the effect of the relative location of the two parallel faults on the consecutive rupturing and the results.

relative location	fault distance	result	Figure
left step of 0.75 km	0 km	consecutive rupture	-
	2 km	consecutive rupture	Fig. 9(b)
	5 km	single rupture	Fig. 9(a)
	10 km	single rupture	-
right step of 0.75 km	0 km	consecutive rupture	-
	2 km	consecutive rupture	-
	5 km	consecutive rupture	Fig. 9(c)
	10 km	single rupture	Fig. 9(d)

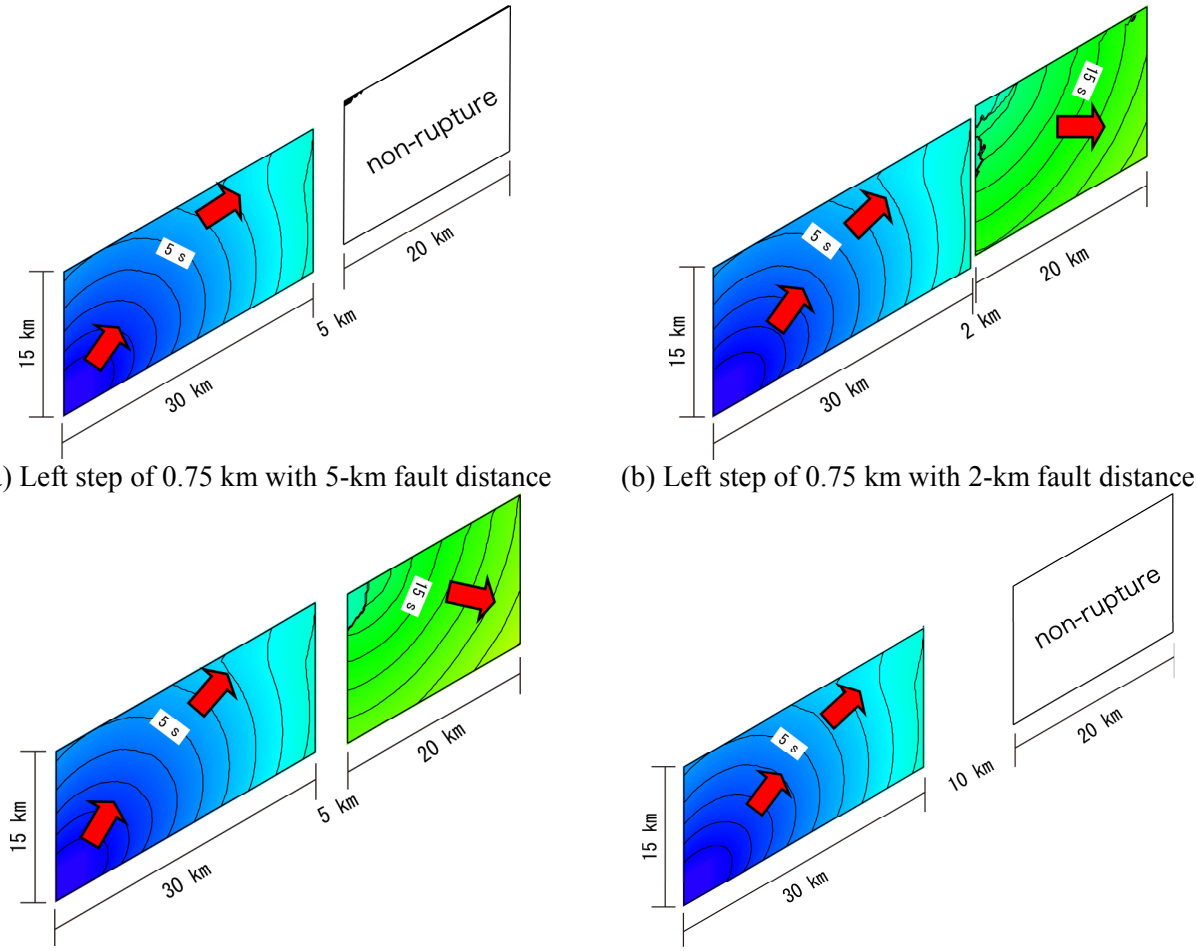

(a) Left step of 0.75 km with 5-km fault distance (b) Left step of 0.75 km with 2-km fault distance

(c) Right step of 0.75 km with 5-km fault distance (d) Right step of 0.75km with 10-km fault distance

Fig. 9. The effect of the relative location of the two parallel faults on the consecutive rupturing.

6. CONCLUSIONS

We examined several series of adjacent faults to find out the conditions of the consecutive rupturing by the numerical dynamic simulation. We obtained the following conclusions:

1) Even if the distance between the adjacent faults was larger, the consecutive rupturing occurred when the strength excess of the fault was small enough.
2) As the width of the inactive area became narrower and the negative stress drop on the inactive area became smaller, the consecutive rupturing of the fault occurred more easily. When the consecutive rupture occurred, the inactive area also ruptured at the same time.
3) Since the rupture of the first left-lateral fault decreased the compressional normal stress on the right-step adjacent fault, the right-step adjacent fault ruptured easily than the left-step adjacent fault.

REFERENCES

Andrews, D. J. (1976) Rupture velocity of plane strain shear cracks. *Journal of Geophysical Research*, **81**, 5679-5687.

Aochi, H., and Fukuyama, E. (2002) Three-dimensional nonplanar simulation of the 1992 Landers earthquake. *Journal of Geophysical Research*, **107:B2**, doi:10.1029/2000JB000061.

Aochi, H. and Ide, S. (2004) Numerical study on multi-scaling earthquake rupture. *Geophysical Research Letters*, **31:2** 10.1029/2003GLO18708.

Eshelby, J. D. (1957) The determination of the elastic field of an ellipsoidal inclusion, and related problems. *Proceedings of the Royal Society of London*, Series A, **241**, 376-396.

Fukuyama, E., Mikumo, T. and Olsen, K. B. (2003) Estimation of the critical slip-weakening distance: Theoretical back ground. *Bulletin of the Seismological Society of America*, **93:4**, 1835-1840.
Irikura, K. and Miyake, H. (2001) Prediction of strong ground motion for scenario earthquake. *Journal of Geography*, **110:6**, 849-875(in Japanese).
Kase, Y. and Kuge, K. (2001) Rupture propagation beyond fault discontinuities: Significance of fault strike and location. *Geophysical Journal International*, **147**, 330-342.
Kase Y. (2002) Rupture propagation beyond fault discontinuities: effect of depth-dependent stress. *Journal of Geography*, **111:2**, 287-297(in Japanese with English abstract).
Kase, Y. and Day, S. M. (2006) Spontaneous rupture processes on a bending fault, *Geophysical Research Letters*, **33,** doi 10. 1029/2006GL025870.
Mikumo, T. Olsen, K. B., Fukuyama, E. and Yagi, Y. (2003) Stress-breakdown time and slip-weakening distance inferred from slip-velocity functions on earthquake faults. *Bulletin of the Seismological Society of America*, **93:1**, 264-282.
Piatanesi, A., Tinti., E., Cocco, M. and Fukuyama, E. (2004) The dependence of traction evolution on the earthquake source time function adopted in kinematic rupture models. *Geophysical Research Letters*, **31**, L04609, 10.1029/2003GL019225.